Novel InAs/GaSb/AlSb tunnel structures

David H. Chow, Jan Soederstroem, D. A. Collins, David Z. Y. Ting, Edward T. Yu, et al.

David H. Chow, Jan Soederstroem, D. A. Collins, David Z.Y. Ting, Edward T. Yu, Thomas C. McGill, "Novel InAs/GaSb/AlSb tunnel structures," Proc. SPIE 1283, Quantum Well and Superlattice Physics III, (1 October 1990); doi: 10.1117/12.20765

SPIE.

Event: Advances in Semiconductors and Superconductors: Physics Toward Devices Applications, 1990, San Diego, CA, United States

Invited Paper

Novel InAs/GaSb/AlSb tunnel structures

D.H. Chow, J.R. Söderström, D.A. Collins,
D.Z.-Y. Ting, E.T. Yu and T.C. McGill

California Institute of Technology
Pasadena, California 91125

ABSTRACT

The nearly lattice–matched InAs/GaSb/AlSb system offers tremendous flexibility in designing novel heterostructures due to its wide range of band alignments. We have recently exploited this advantage to demonstrate a new class of negative differential resistance (NDR) devices based on interband tunneling. We have also studied "traditional" double barrier (resonant) and single barrier NDR tunnel structures in the InAs/GaSb/AlSb system. Several of the interband and resonant tunneling structures display excellent peak current densities (as high as 4×10^5 A/cm^2) and/or peak–to–valley current ratios (as high as 20:1 and 88:1 at 300 K and 77 K, respectively), offering great promise for high frequency and logic applications.

1. INTRODUCTION

Quantum mechanical tunneling of charge carriers in semiconductor heterostructures continues to be a subject of great interest. Much of the motivation for studying tunnel structures stems from their potential high frequency analog applications.[1] For example, a 420 GHz oscillator was recently demonstrated using a GaAs/AlAs resonant tunneling diode.[2] It has also been proposed that three terminal devices incorporating GaAs/AlAs tunnel structures could have advantages in digital applications via multiple level logic.[3]

In spite of the progress that has been made with GaAs/AlAs (and $Al_xGa_{1-x}As$) resonant tunneling structures, it has become clear that fundamental limitations exist on their performance. Maximum peak current densities of approximately 1.5×10^5 A/cm^2 can be reached only by reducing room temperature peak–to–valley ratios to 2:1 or less.[2,4] Further improvements seem unlikely because of inherently poor GaAs ohmic contacts and low indirect conduction band minima in the AlAs barriers. The nearly lattice–matched InAs/GaSb/AlSb material system would seem to be an attractive alternative to GaAs/AlAs because of its flexibility for tunnel structure design. Fig. 1 displays the band edges of the three materials, using recent band offset data.[5,6] In addition to the obvious flexibility enhancement derived from having three materials from which to choose, this material system allows for the possibility of staggered and broken–gap band alignments. Furthermore, the InAs/AlSb conduction band offset is substantially higher than that of GaAs/AlAs (referring to the indirect conduction band minima in AlSb and AlAs). Finally, InAs and GaSb are excellent materials for n–type and p–type ohmic contacts, respectively.

In this paper, we present experimental results from several InAs/GaSb/AlSb tunnel structures. Several of these new heterostructures are superior to the best GaAs/AlAs double barriers in terms of peak current densities and/or peak–to–valley current ratios. The tunnel structures can be divided into three classes, based upon the mechanisms through

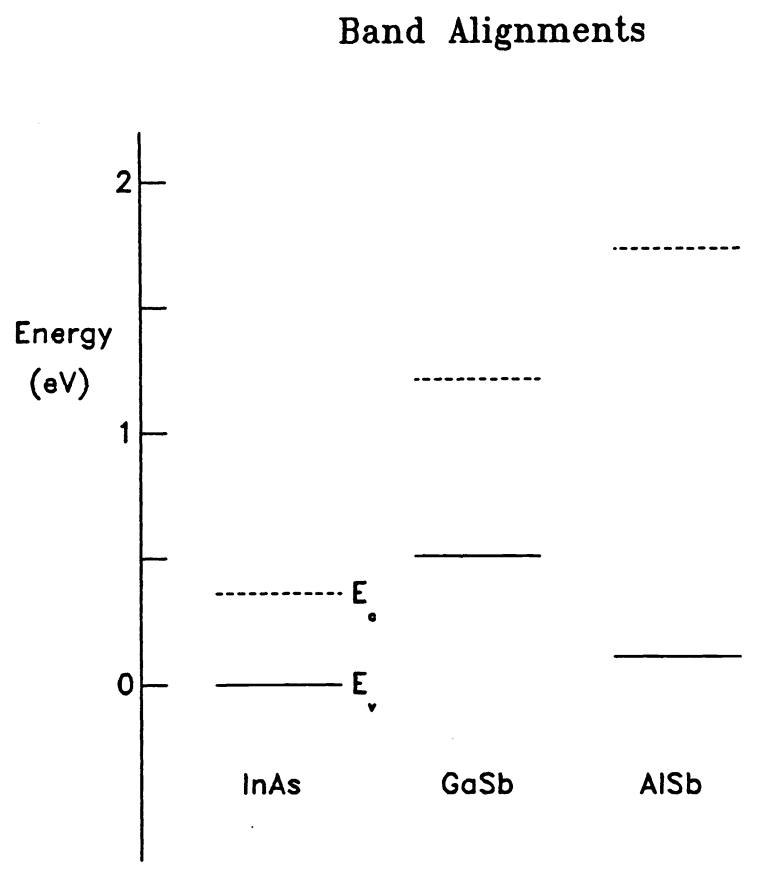

Fig. 1. Conduction (dashed) and valence (solid) band edges of InAs, GaSb, and AlSb. Band offsets values have been taken from recent x–ray photoemission reports.[5,6]

which they produce negative differential resistance (NDR): "conventional" resonant tunneling, single barrier (simple elastic) tunneling, and resonant interband tunneling. In the first category, InAs/AlSb double barrier heterostructures have been shown to yield peak current densities and peak–to–valley current ratios superior to those obtainable from GaAs/AlAs (or GaAs/$Al_xGa_{1-x}As$) double barriers. The other two categories of tunnel structures result directly from the staggered (InAs/$Ga_{1-x}Al_xSb$) and broken–gap (InAs/GaSb) band alignments afforded by this material system. In the case of the resonant interband tunneling devices, extremely high peak–to–valley curent ratios with reasonable peak current densities have been observed.

2. EXPERIMENTAL

2.1. Growth

All of the tunnel structures studied have been grown by molecular beam epitaxy (MBE) on (100)–oriented GaAs substrates. The Perkin Elmer 430 MBE system is equipped with cracked As and Sb sources, which produce dimeric molecular beams of the two materials

(As_2 and Sb_2). Substrate temperatures above 500°C were monitored with an optical pyrometer, calibrated to the GaAs oxide desorption temperature and the As–stabilized to In–stabilized transition in the surface reconstruction of InAs. A thermocouple in contact with a molybdenum block, to which the substrate was bonded with indium, was used to estimate temperatures below 500°C.

The InAs/GaSb/AlSb heterostructures were deposited on thick, strain–relaxed buffer layers of InAs or GaSb, depending upon whether InAs(n^+) or GaSb(p^+) electrodes were desired. In both cases, a short period, heavily strained superlattice was grown at the GaAs/buffer layer interface to reduce the number of threading dislocations in the buffer layer.[7,8] For InAs electrodes, growth commenced with 3000 Å of GaAs at a substrate temperature of 600°C, followed by a five period, 2 monolayer/2 monolayer, $In_{0.7}Ga_{0.3}As$/GaAs superlattice at 520°C, and a 5000 Å thick InAs(n^+) layer grown at 500°C. GaSb buffer layers consisted of 3000 Å of GaAs grown at 600°C, followed by a 1 monolayer/1 monolayer, GaAs/GaSb superlattice at 520°C, and a 5000 Å thick GaSb(p^+) layer grown at 470°C. Some structural characterization of the buffer layers has been reported elsewhere.[9] Doping of the electrodes (n–type for InAs, p–type for GaSb) was achieved by codeposition of silicon during growth. It has recently been demonstrated that GaSb can be controllably doped p–type with silicon under the growth conditions described above.[10] For some of the tunnel structures, lightly doped ($n \approx 5 \times 10^{16}$ cm^{-3} or $p \approx 5 \times 10^{16}$ cm^{-3}) and/or undoped spacer layers sandwiched the barrier and quantum well layers. Reflection high energy electron diffraction patterns observed during growth revealed a 2×4 surface reconstruction for InAs, and 1×3 reconstructions for GaSb, AlSb, and $Ga_{1-x}Al_xSb$.

2.2. Device fabrication

Conventional photolithographic and chemical etching techniques have been used to define mesas ranging in size from 2 μm diameter circles to 70×160 μm rectangles. Samples with InAs electrodes were etched in H_2SO_4:H_2O_2:H_2O (1:8:80), while Br_2:HBr:H_2O (0.5:100:100) was used to etch GaSb electrodes. In most cases, electrical contacts were formed by depositing Au/Ge on the mesas and etched surface. We have also tested Al contacts to GaSb(p^+) electrodes, and *in situ* In (prior to removal from the MBE) contacts to InAs(n^+) electrodes with good results. Current–voltage characteristics were measured with a Tektronics 577 curve tracer and/or an HP4145 analyzer, by probing the mesas with a 25 μm diameter Au wire.

3. CONVENTIONAL RESONANT TUNNELING

GaAs/AlGaAs double barrier heterostructures have been studied extensively as potential high frequency devices.[2,4] However, the performance of these GaAs/AlGaAs structures appears to be limited by poor ohmic contacts and the loss of NDR at high current densities. InAs/AlSb double barrier heterostructures are expected to have significant advantages over GaAs/AlGaAs structures because, (*i*) n–type InAs is ideal for ohmic contacts, and (*ii*) the InAs/AlSb conduction band offset (InAs Γ–point to AlSb X–point) is much larger than that of GaAs/AlAs (GaAs Γ–point to AlAs X–point) or GaAs/$Al_{0.4}Ga_{0.6}As$ (GaAs Γ–point to $Al_{0.4}Ga_{0.6}As$ Γ–point). NDR in InAs/AlSb double barrier heterostructures was first demonstrated by Luo *et al.*[11] with moderate peak–to–valley ratios and current densities. More

recently, we have observed peak–to–valley ratios of 11:1 at room temperature at a peak current density of 4×10^3 A/cm^2, as shown in Fig. 2.[12] The curve displayed in Fig. 2 was obtained from a heterostructure which consisted of a 65 Å InAs quantum well sandwiched between 28 Å AlSb barriers, 50 Å undoped InAs spacer layers, and 500 Å lightly doped ($n \approx 2 \times 10^{16}$ cm^{-3}) InAs spacer layers. The electrodes consisted of thick, heavily doped InAs layers, with $n \approx 1 \times 10^{18}$ cm^{-3}.

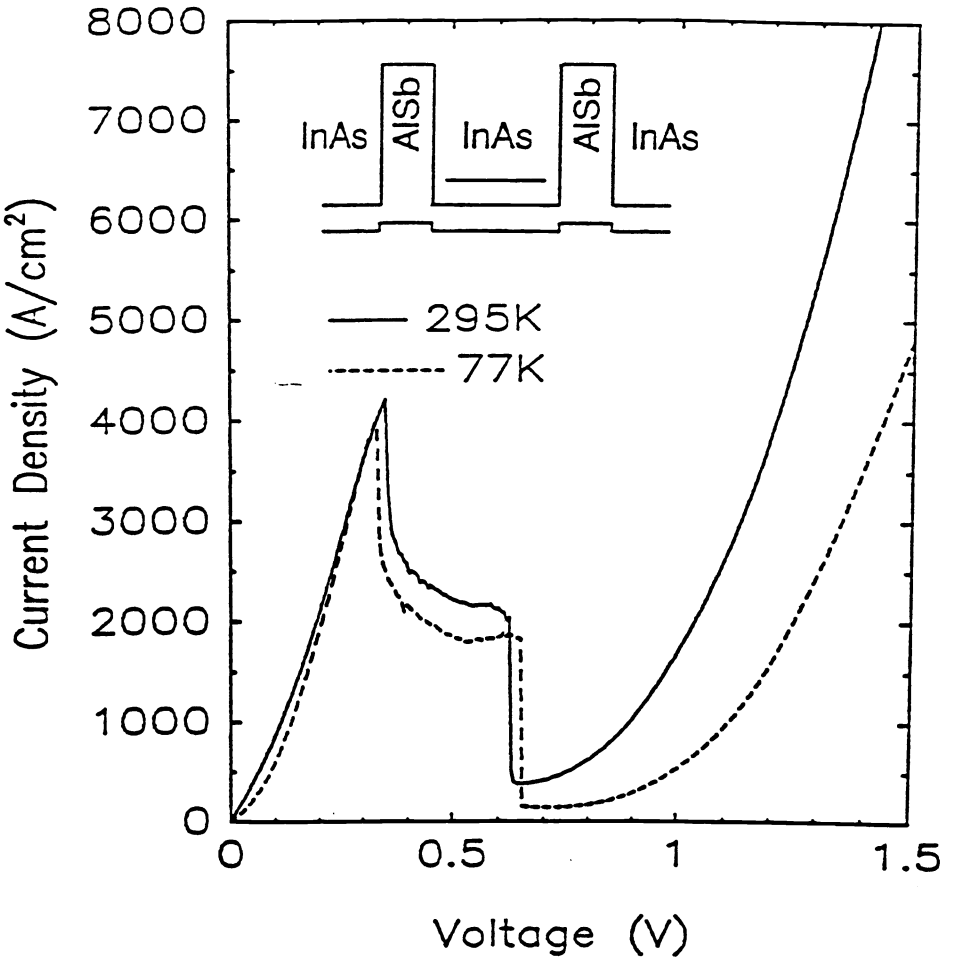

Fig. 2. Experimental current density vs. voltage curve, taken from an InAs/AlSb double barrier heterostructure with 28 Å barriers.

Although a trade–off between peak–to–valley ratios and current densities exists for InAs/AlSb resonant tunneling structures (as for GaAs/AlGaAs structures), reasonably high values for both figures of merit have been achieved. For example, we have observed a peak–current density of 4×10^5 A/cm^2 with a peak–to–valley ratio of 4:1 from a sample with 4 monolayer AlSb barriers and an asymmetric doping profile.[13] In terms of high frequency analog applications, these values are significantly better than the best GaAs/AlGaAs results reported. Thus, it is likely that InAs/AlSb resonant tunneling structures can be used as

microwave oscillators at frequencies significantly higher than 420 GHz, the highest frequency reported for GaAs/AlGaAs resonant tunneling devices.[2]

4. SINGLE BARRIER NDR

It has been proposed[14,15] and demonstrated[16-19] that single barrier tunnel structures can exhibit NDR in certain material systems. The basic requirement for observation of single barrier NDR is that tunneling electrons (holes) lie much closer in energy to the valence (conduction) band edge in the barrier material than to the conduction (valence) band edge. This requirement can be satisfied by electrons tunneling from InAs(n) electrodes into an $Al_xGa_{1-x}Sb$ barrier for $x \approx 0.4$, as depicted in Fig. 3. The single barrier structure can yield NDR because the electron tunneling probability is reduced as the valence band edge in the $Al_xGa_{1-x}Sb$ barrier is pushed to lower energies (with respect to the tunneling electrons) by an increasing applied voltage.

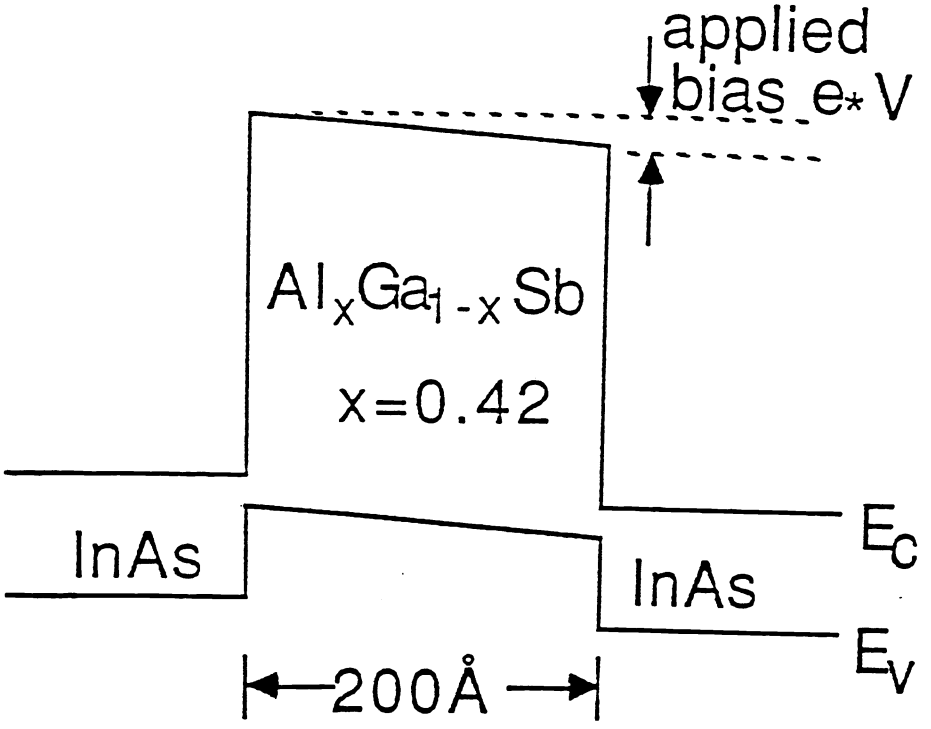

Fig. 3. Band–edge diagram for an InAs(n)/$Al_{0.42}Ga_{0.58}Sb$ single barrier heterostructure under an applied bias.

Fig. 4 contains room temperature and 77 K current density vs. voltage (J–V) curves from a single barrier InAs/$Al_{0.42}Ga_{0.58}Sb$ heterostructure. A room temperature (77 K) peak–to–valley current ratio of 1.2 (3.4) is observed in reverse bias (negative voltage on the mesa), at a modest current density ($\approx$ 25 A/cm^2). The J–V curves were taken from a structure which consisted of a 200 Å $Al_{0.42}Ga_{0.58}Sb$ barrier sandwiched between 100 Å undoped InAs spacer

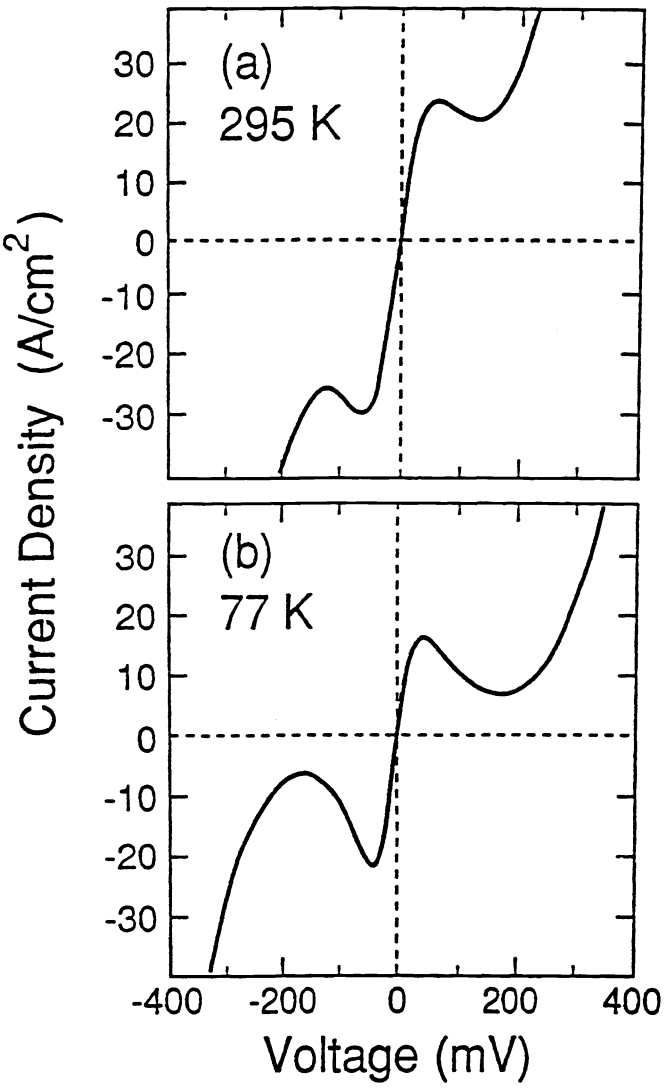

Fig. 4. Experimental current density vs. voltage curve at (a) room temperature and (b) 77 K for an InAs(n)/$Al_{0.42}Ga_{0.58}Sb$ single barrier heterostructure.

layers, and 500 Å lightly doped ($n \approx 2 \times 10^{16}$ cm^{-3}) spacer layers. The electrodes consisted of thick, heavily doped InAs layers, with $n \approx 1 \times 10^{18}$ cm^{-3}.

It is interesting to note that the J–V curves shown in Fig. 4 do not display threshold voltages for tunneling because single barrier elastic tunneling is allowed at any applied bias (in contrast to resonant tunneling). The peak in the J–V curve occurs when additional incident electrons in the negatively biased electrode are no longer generated by an increasing bias (approximately when the voltage surpasses the Fermi level in the spacer layers). We have also demonstrated NDR in this material system for single $Al_xGa_{1-x}Sb$ barrier compositions of $x = 0.38$, 0.40, and 0.44.[19]

5. RESONANT INTERBAND TUNNELING

Resonant interband tunneling (RIT) structures have recently been proposed[20] and demonstrated[21,22]. In these structures, electrons (holes) in one material tunnel through a quasi–bound valence (conduction) band state in a different material. This mechanism yields a drastic suppression of valley currents due to the blocking nature of the quantum well layer past resonance. We have observed peak–to–valley current ratios as large as 20:1 (88:1) at 300 K (77 K) from an InAs(n)/AlSb/GaSb/AlSb/InAs(n) (n–type InAs electrodes, AlSb barriers, and a GaSb quantum well) RIT structure.[21]

We report here an experimental and theoretical study of the current–voltage behavior of a GaSb(p)/AlSb/InAs/AlSb/GaSb(p) heterostructure. Fig. 5 contains a band–edge diagram for the heterostructure. The crucial feature of the diagram is that the conduction band edge in the InAs quantum well is *lower* in energy than the valence band edge in the GaSb electrodes. The InAs layer has been grown sufficiently thick to keep the quantum well ground state below the GaSb valence band maximum. Due to the strong coupling between conduction band and light hole states, a transmission resonance exists for light holes in the GaSb electrodes whose energies and parallel wavevectors match those of states in the two dimensional quantum well subband. It is straightforward to show that this resonance condition can be satisfied for small applied biases (no threshold voltage). A peak in the I–V curve is expected when the applied bias becomes large enough to lower the valence band edge in the positively biased GaSb electrode below the ground state energy in the InAs quantum well. Beyond this point, the tunneling probability is drastically reduced due to the blocking nature of the thick InAs layer at energies in its band gap. It should be noted that heavy holes are not expected to contribute significantly to the tunneling current because they are weakly coupled to conduction band states.

We have developed a theoretical model to simulate the current–voltage behavior of tunnel structures in which interactions between valence and conduction band states are important. The simulation begins by computing the band edge diagram throughout the heterostructure via the Poisson equation for each applied bias. In the case of the RIT structure studied here, the heavy hole band dominates the band bending behavior in the GaSb electrodes because its density of states is fifteen times greater than that of the light hole band. Next, localized two–band tight–binding orbitals are used to generate transfer matrices for the tunneling states. In this manner, a transmission coefficient is determined as a function of the energy and parallel wavevector of each state. In our model, only the conduction and light hole bands are used to determine the tight–binding parameters for each material. The restriction to these two bands is effectively an assumption that only electron–light hole coupling is significant in the tunnel structure (heavy hole tunneling is ignored). Finally, the current density is obtained by including appropriate velocities and Fermi factors and integrating over all energies and parallel wavevectors.

MBE growth and device fabrication have been performed as described in Section 2. The active region of the structure consisted of a 100 Å InAs quantum well, sandwiched between 20 Å AlSb barriers, 25 Å undoped GaSb spacer layers, and 200 Å lightly doped ($p \approx 2 \times 10^{16}$ cm^{-3}) GaSb spacer layers. The electrodes consisted of thick, heavily doped GaSb layers, with $p \approx 5 \times 10^{18}$ cm^{-3}.

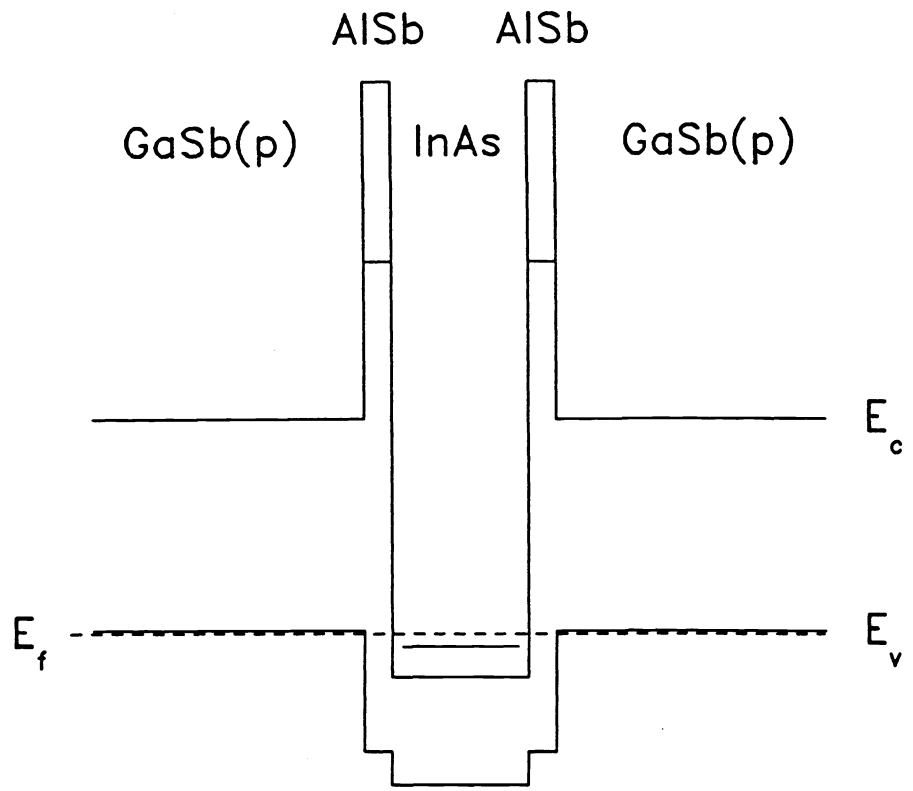

Fig. 5. Schematic band–edge diagram (energy vs. position) for the GaSb(p)/AlSb/InAs/AlSb/GaSb(p) RIT heterostructure. The conduction band edge, E_c, valence band edge, E_v, and Fermi energy, E_f, are labeled. The indirect (lower) and direct (higher) conduction band edges are both shown in the AlSb layers. The position of the quasi–bound state in the InAs quantum well is also shown.

Fig. 6 displays a current density vs. voltage curve taken at 300 K from one of the fabricated devices. Also plotted are theoretical curves, calculated by the method described previously, for symmetric 6 and 7 monolayer (18.4 and 21.5 Å) AlSb barrier layers. The experimental curve shows pronounced NDR in both bias directions, with peak–to–valley current ratios of 8.3 and 3.6 in reverse and forward bias, respectively (we take forward bias to mean positive voltage applied to the mesa). The peak current density is 430 A/cm^2 (560 A/cm^2) in reverse (forward) bias, and varied by less than 15% over ten randomly chosen devices.

As shown in Fig. 6, the peak current densities predicted by the theoretical model are in good agreement with those measured experimentally. It has been suggested that the high scattering rate of heavy holes in bulk GaSb to the light hole band results in identical tunneling probabilities for the two types of carriers.[22] If this were the case, we would expect the large heavy hole density of states to yield measured peak current densities greater than our theoretically predicted value by more than one order of magnitude. Thus, the observed agreement between the experimental and theoretical current densities suggests that heavy

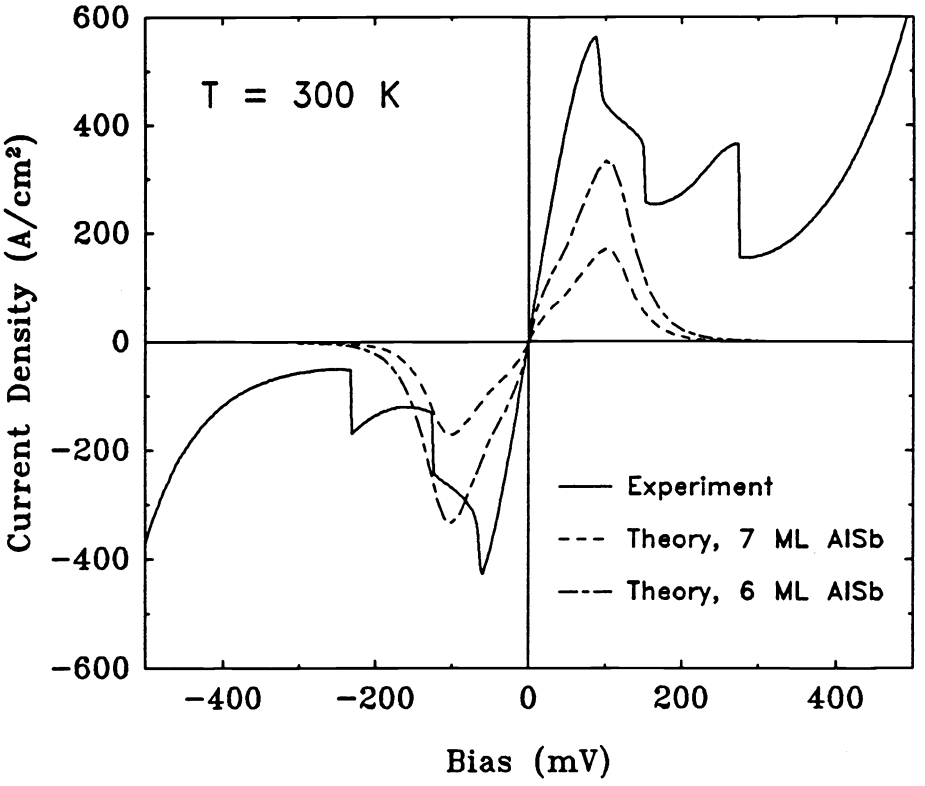

Fig. 6. Experimental current density vs. voltage curve taken from the GaSb(p)/AlSb/InAs/AlSb/GaSb(p) RIT device. Also displayed are theoretically simulated curves, calculated for 6 and 7 monolayer (ML) AlSb barrier layers. The theoretical model includes only light hole contributions to the resonant interband tunneling current.

hole tunneling probabilities are small. The experimental curve shown in Fig. 6 displays some asymmetry, with the forward bias peak appearing 20 mV higher than the reverse bias peak. This feature is probably caused by unintentional asymmetries in the doping profile of the device, introduced during growth. It should be noted that the observed valley currents are significantly higher than the calculated values, suggesting that transport mechanisms other than elastic tunneling dominate the current at high bias.

In addition to the demonstration of high peak–to–valley current ratios in RIT devices, we have recently explored interband tunneling devices designed to yield high peak current densities. Each of these heterostructures consists of an undoped GaSb quantum well ($\approx$ 150 Å thick) sandwiched between heavily doped InAs(n^+) electrodes.[23] The major difference between this structure and the RIT's described previously is the absence of AlSb barriers. Nevertheless, a quasi–bound state is formed in the GaSb quantum well due to non–negligible reflections of the free carrier wavefunctions at the InAs/GaSb interfaces. This quantum well state results in a transmission resonance for electrons in the InAs electrodes whose energies and parallel wavevectors match those of states in the two dimensional quantum well subband.

We have observed peak current densities in excess of 2×10^4 A/cm^2 from these structures, with peak–to–valley current ratios of 2:1.[23] These results suggest that interband tunneling devices may be suitable for high frequency applications. Furthermore, the quasi–bound states in the barrierless RIT's are extremely broad, due to the extremely weak confinement. As a result, the tunneling time in these structures, as defined by the uncertainty principle relating the energy width of the resonanance to the lifetime of the quasi–bound state, is very short ($\approx$ 50 fs), and should not be the limiting factor in the frequency of operation.

6. CONCLUSIONS

In summary, we have studied several novel InAs/GaSb/AlSb tunnel structures. This material system offers several advantages over GaAs/AlGaAs for tunnel structure design: (*i*) enhanced flexibility from *three* nearly–lattice matched materials, (*ii*) the possibility of staggered and broken–gap band alignments, (*iii*) large conduction band offsets, and (*iv*) excellent ohmic contacts. We have studied three distinct mechanisms for achieving negative differential resistance from InAs/GaSb/AlSb structures: conventional resonant tunneling, single barrier tunneling, and resonant interband tunneling. Several of the structures show extremely high peak current densities and/or peak–to–valley current ratios. These results suggest that the InAs/GaSb/AlSb material system is ideal for fabrication of high frequency oscillators and mixers.

7. ACKNOWLEDGEMENTS

The authors gratefully acknowledge helpful discussions with Y. Rajakarunanayake, M.K. Jackson, and E.R. Brown. The support of the Office of Naval Research and the Air Force Office of Scientific Research under Grant Nos. N00014–89–J–1141 and AFOSR–86–0306, respectively, have made it possible for us to carry out this program. J.R. Söderström received financial support from the Wilhelm and Martina Lundgren Foundation. E.T. Yu was supported in part by the AT& T Foundation. D.H. Chow was supported in part by Caltech's Program in Advanced Technologies, sponsored by Aerojet General, General Motors, and TRW.

8. REFERENCES

1. K.A. Lee and M.A. Frerking, "Experimental results of a high Q quasioptical reflection cavity," Int. Journal of Infrared and Millimeter Waves, vol. 10, no. 7, pp. 789–802, 1989.
2. E.R. Brown, T.C.L.G. Sollner, C.D. Parker, W.D. Goodhue, and C.L. Chen, "Oscillations up to 420 GHz in GaAs/AlAs resonant tunneling diodes," Appl. Phys. Lett., vol. 55, no. 17, pp. 1777–1779, 1989.
3. F. Capasso, S.Sen, A.Y. Cho, and D.L. Sivco, "Multiple negative transconductance and differential conductance in a bipolar transistor by sequential quenching of resonant tunneling," Appl. Phys. Lett., vol. 53, no. 12, pp. 1056–1058, 1988.
4. S.K. Diamond, E. Özbay, M.J.W. Rodwell, D.M. Bloom, E. Wolak, and J.S. Harris, "Fabrication of 200–GHz f_{max} resonant–tunneling diodes for integrated circuit and microwave applications," IEEE Elec. Dev. Lett., vol. 10, no. 3, pp. 104–106, 1989.

5. G.J. Gualtieri, G.P. Schwartz, R.G. Nuzzo, R.J. Malik, and J.F. Walker, "Determination of the (100) InAs/GaSb heterojunction valence–band discontinuity by x–ray photoemission core level spectroscopy," J. Appl. Phys., vol. 61, no. 12, pp. 5337–5341, 1987.
6. G.J. Gualtieri, G.P. Schwartz, R.G. Nuzzo, and W.A. Sunder, "X–ray photoemission core level determination of the GaSb/AlSb heterojunction valence–band discontinuity,"Appl. Phys. Lett., vol. 49, no. 16, pp. 1037–1039, 1986.
7. S. Kalem, J.I. Chyi, H. Morkoc, R. Bean, and K. Zanio, "Growth and transport properties of InAs epilayers on GaAs," Appl. Phys. Lett., vol. 53, no. 17, pp. 1647–1649, 1988.
8. J.R. Söderström, D.H. Chow, and T.C. McGill, "MBE–growth of InAs and GaSb epitaxial layers on GaAs substrates," Mat. Res. Soc. Symp. Proc., vol. 145, pp. 409–414, 1989.
9. D.H. Chow, R.H. Miles, J.R. Söderström, and T.C. McGill, "InAs/$Ga_{1-x}In_xSb$ strained–layer superlattices grown by molecular beam epitaxy," to appear in *J. Vac. Sci. and Technol. B*, July/August 1990.
10. T.M. Rossi, D.A. Collins, D.H. Chow, and T.C. McGill, "P–type doping of gallium antimonide grown by molecular beam epitaxy using silicon," unpublished.
11. L.F. Luo, R. Beresford, and W.I. Wang, "Resonant tunneling in AlSb/InAs/AlSb double–barrier heterostructures," Appl. Phys. Lett. vol. 53, no. 23, pp. 2320–2322, 1988.
12. J.R. Söderström, D.H. Chow, and T.C. McGill, "InAs/AlSb double–barrier structure with large peak–to–valley current ratio: a candidate for high–frequency microwave devices," IEEE Elec. Dev. Lett., vol. 11, no. 1, pp. 27–29 1990.
13. J.R. Söderström, T.C. McGill, and E.R. Brown, unpublished.
14. G.A. Sai–Halasz, R. Tsu, and L. Esaki, "A new semiconductor superlattice," Appl.Phys.Lett., vol. 30, no. 12, pp. 651–653, 1977.
15. D.H. Chow and T.C. McGill, "Negative differential resistances from $Hg_{1-x}Cd_xTe$ single quantum barrier heterostructures," Appl. Phys. Lett., vol. 48, no. 21. pp. 1485–1487, 1986.
16. D.H. Chow, T.C. McGill, I.K. Sou, J.P. Faurie, and C.W. Nieh, "Observation of negative differential resistance from a single barrier heterostructure," Appl. Phys. Lett., vol. 52, no. 1, pp. 54–56, 1988.
17. H. Munekata, T.P. Smith III, and L.L. Chang, "Growth and transport properties of (Ga,Al)Sb barriers on InAs," J. Vac. Sci. Technol. B, vol. 7, pp. 324–326, 1989.
18. R. Beresford, L.F. Luo, W.I. Wang, "Negative differential resistance in AlGaSb/InAs single barrier heterostructures at room temperature," Appl. Phys. Lett., vol. 54, no. 19, pp. 1899–1901, 1989.
19. J.R. Söderström, D.H. Chow, and T.C. McGill, "Demonstration of large peak–to–valley current ratios in InAs/AlGaSb/InAs single–barrier heterostructures," Appl. Phys. Lett., vol. 55, no. 13, pp. 1348–1350 1989.
20. M. Sweeny and J. Xu, "Resonant interband tunnel diodes," Appl. Phys. Lett., vol. 54, no. 6, pp. 546–548, 1989.
21. J.R. Söderström, D.H. Chow, and T.C. McGill, "New negative differential resistance device based on resonant interband tunneling," Appl. Phys. Lett., vol. 55, no. 11, pp. 1094–1096, 1989.

22. L.F. Luo, R. Beresford, and W.I. Wang, "Interband tunneling in polytype GaSb/AlSb/InAs heterostructures," Appl. Phys. Lett., vol. 55, no. 19, pp. 2023–2025, 1989.
23. D.A. Collins, D.H. Chow, and T.C. McGill, "Observation of negative differential resistance in a broken–gap resonant interband tunneling structure," unpublished.